PASSIVE INTENSITY MODULATION OF LIGHT USING A DIGITAL MICROMIRROR DEVICE IN A MICROSCALE SELECTIVE LASER SINTERING SYSTEM FOR ENHANCED PART UNIFORMITY

A. Liao[1], J. Grose[1], H. Kim[2], M. A. Cullinan[1], C. Okwudire[2]

[1]Walker Department of Mechanical Engineering, The University of Texas at Austin, Austin, TX
[2]Department of Mechanical Engineering, University of Michigan, Ann Arbor, MI

Abstract

Microscale selective laser sintering (μ-SLS) aims to fabricate sub-5 μm features with a high throughput for the advanced semiconductor packaging industry, where fine resolution features are required. In μ-SLS, a metal nanoparticle bed is heated with laser projection masks from a digital micromirror device (DMD). As sintering progresses, unwanted heat conduction to areas outside of the mask occurs, reducing process resolution. Optical vignetting and DMD defects produce nonuniform intensity across the frame. A beam profiler was used to determine a field correction for spatial nonuniformity across the projected area. This was combined with a temperature profile generated from a pre-existing nanoparticle bed sintering FEA simulation to develop an optical mask to improve temperature uniformity across the sintering bed. Future work includes combining these passive correction approaches with a control framework based on nanoparticle bed sintering models to optimize the thermal profile through displaying a sequence of patterns instead of a static corrected image.

Introduction

The goal of developing the microscale selective laser sintering process is to produce three-dimensional components with sub-5 μm features, at a throughput of ~ 50 mm³/hr [1]. To form each layer, the process heats a nanoparticle bed at a specific location, applies a fresh layer of nanoparticles onto the sintered surface, and precisely aligns the components between each added layer. The current machine version includes three main subsystems to accomplish this: an optical sintering system, global and nanopositioning systems, and a nanoparticle ink dispensing system, as shown below.

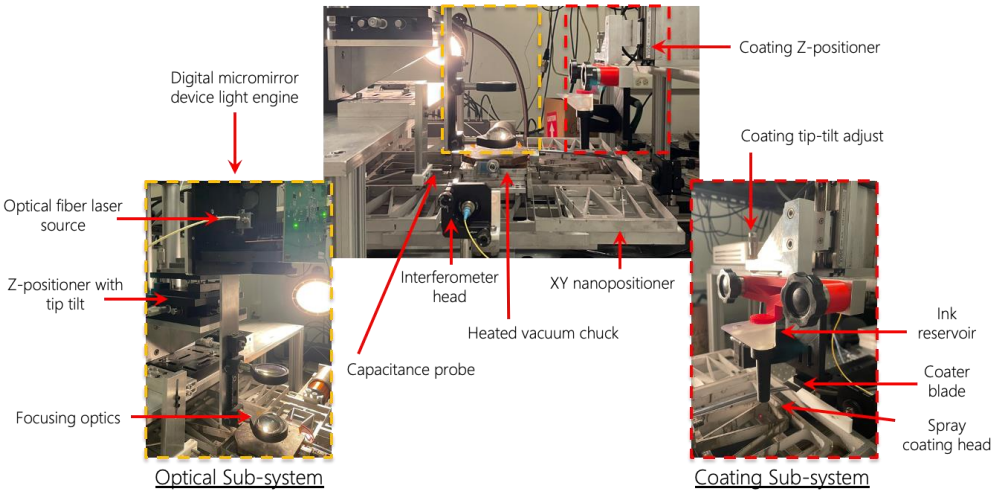

Figure 1: Diagram showing the subsystems of the microscale selective laser sintering machine and their sub-components.

The process begins by coating a substrate with a thin layer of nanoparticle ink with the coating subsystem. A long stroke linear motor moves the substrate underneath the sintering station which uses a digital micromirror device to project a pattern with an 808 nm wavelength quasi-continuous wave laser, heating up the particle bed and selectively fusing desired regions. The focusing lens setup allows for each mirror on the DMD to be focused down to a ~1.2 µm spot size, and with an array of 1920 x 1080 mirrors, simultaneous patterning can be performed across a 2.3 x 1.2 mm area. In conjunction with a flexure-based nanopositioning stage, rapid patterning can be performed over a 50 x 50 mm area on the substrate with nanometer precision. After sintering of the current layer is completed, the substrate is then shuttled back to the coating station to form a new bed of nanoparticles above the freshly sintered material. This process is repeated until the desired part geometry is achieved. Excess unsintered nanoparticles surrounding the final parts are then removed by ultrasonication and washing the substrate with solvent. Finally, parts will be thermally annealed to further improve their electrical and mechanical properties.

Background

Previous intensity modulation efforts used the profiles of final parts as a means of correcting for optical defects and thermal gradients [2]. The aim of this work is to instead use beam profiler measurements and temperature prediction from modeling efforts to generate correction profiles. The µ-SLS system currently uses silver and copper metal nanoparticle inks (Novacentrix, Austin, TX) to form the particle bed. Once heated above the material's sintering threshold by incident laser power, the particle ink undergoes a solid-state diffusion process. Since this nanoparticle diffusion process occurs without a phase change, a custom modeling framework is required to predict and account for temperature variations and the evolution of thermal properties within the nanoparticle bed during laser sintering [3], [4]. This custom thermal model allows for temperature gradient prediction which was used for intensity modulation.

Intensity modulation is facilitated by a dedicated light engine, which is a custom microcontroller that interfaces between the host computer and the digital micromirror device (DMD). The light engine utilized in this setup (DLP 6500, Texas Instruments) offers a resolution of 1920 x 1080 pixels and is capable of rendering 10-bit images at a rate of 120 frames per second. This enables modulation of the incident beam into 1024 discrete intensity levels, ranging from zero to full intensity, which can be represented and expressed by greyscale images sent to the microcontroller. This is accomplished by rapidly switching the mirrors between two positions, one where the incident beam is reflected towards a heat sink, and the other towards the nanoparticle bed. The figure below shows schematics of the optical train of the sintering system and a digital micromirror device.

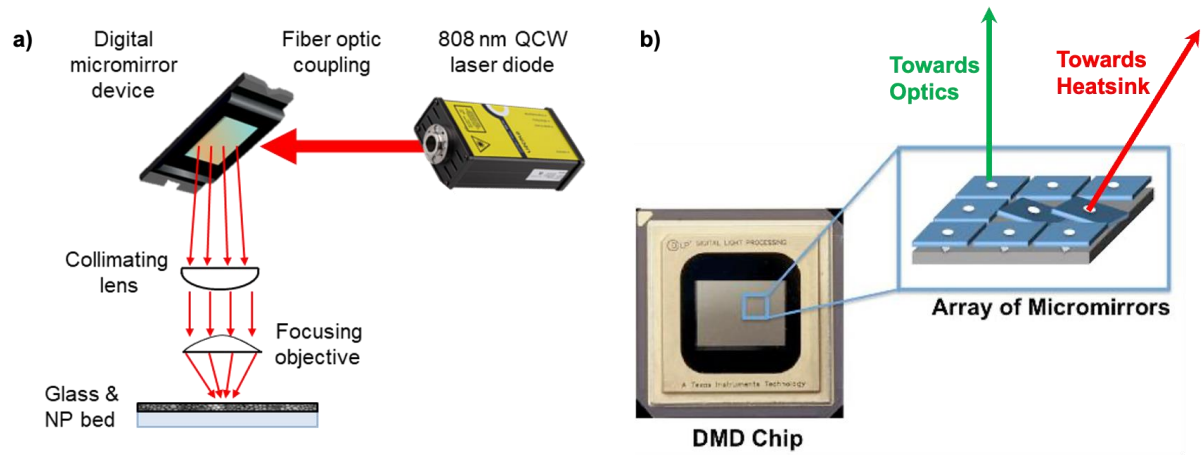

Figure 2: a) Schematic showing the optical path of the laser beginning at the laser diode, reflected off the DMD, through optics, and focused onto the nanoparticle bed. b) Image of DMD chip schematically showing the state of the individual mirrors on the array and reflected beam direction during operation.

A Python script on the host computer displays images in sequence to the DMD, treating it as a second monitor through the DisplayPort protocol. The script selects a folder containing the desired image sequence and displays it on the DMD. This script is synchronized with a LabVIEW program that controls the other operations of the machine, coordinating the laser exposure with the initiation of the image sequence.

While the goal is to fully leverage the spatiotemporal modulation capabilities of the DMD, more complex control methods, combined with precise thermal modeling efforts, must be developed and implemented. Preliminary work on this has been performed on simple shape profiles but has not yet been extended to more complex shapes with finer resolution [5]. The following work focuses on the methods and results of combining two passive correction methods to achieve better temperature and part uniformity across the exposure area of the DMD.

Passive Intensity Correction

A passive intensity correction approach involves projecting a modified static image with varying greyscale intensities with the DMD to modulate optical intensity and compensate for thermal nonuniformity within the particle bed. Any optical nonuniformity, such as vignetting, will reduce the heat generated in less intense areas, so it must be compensated for to achieve even illumination. Additionally, temperature nonuniformity within a particle bed arises under constant laser flux because the thermal properties of the material affect how heat is spread and retained within the bed. Heat spreads less effectively beyond the boundaries of the sintered region, causing the edges of the laser exposure area to remain cooler as the surrounding material dissipates heat.

Optical nonuniformity exists across the frame due to errors in lens alignment, and DMD defects. These can be measured using a beam profiler (Ophir SP90427) with a low power laser. The figure below shows the process of measuring, filtering, and inverting the profile to apply the optical intensity correction.

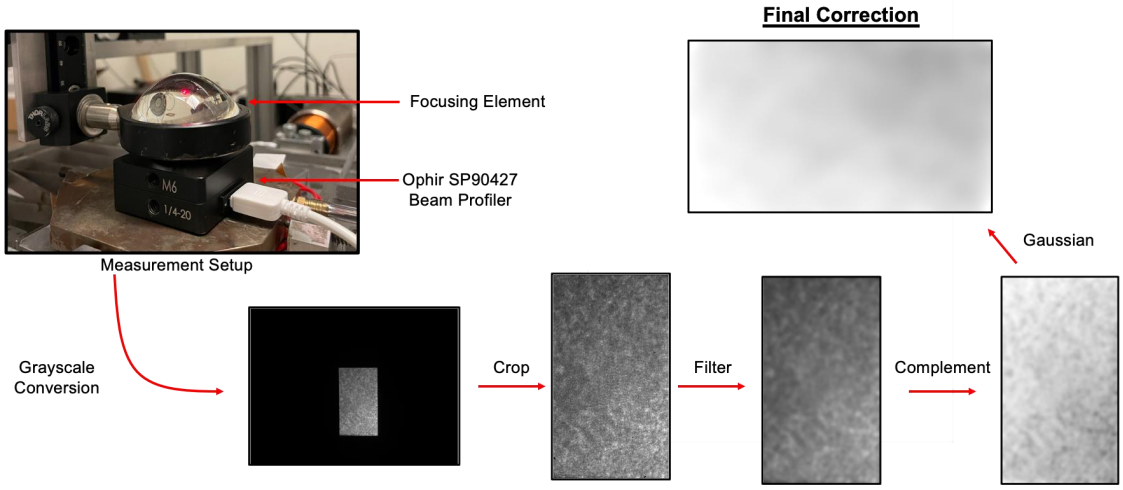

Figure 3: Process of generating the passive optical correction mask. A beam profiler was placed under the focusing optics to measure the intensity distribution of an image with all DMD elements reflecting an incident beam. The resulting image was cropped, filtered, and complemented to produce the final correction mask.

This optical correction can be applied to the desired shape image through element-wise multiplication. It was tested using three different shapes: the base 2.3 x 1.3 mm rectangle, a longhorn shape, and an I shape pattern. Figure 4 below shows the beam profiler intensity distribution for each shape, both before and after correction.

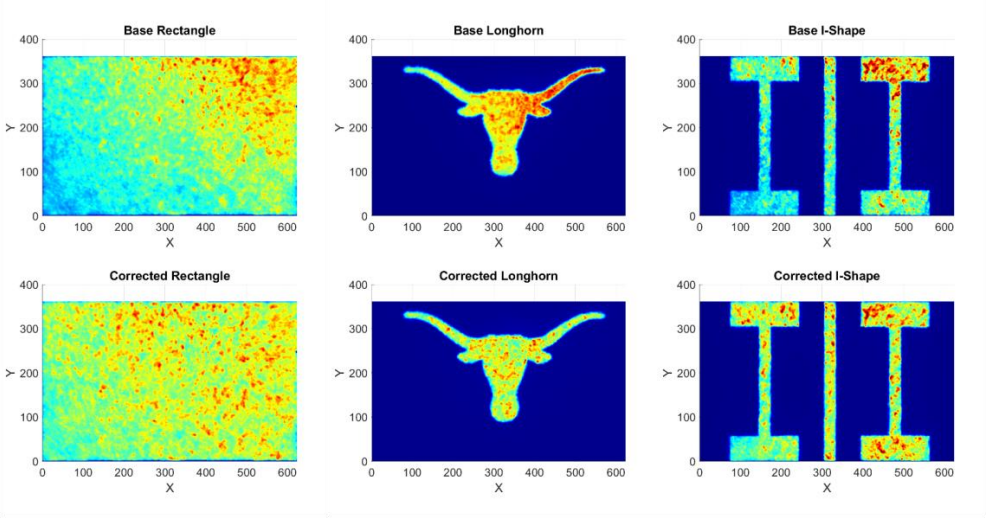

Figure 4: Beam profiler images showing intensity distribution of a rectangle, longhorn, and I-pattern before and after optical correction.

The corrected image has around 80% of the intensity of the unmodulated image, which diminishes the total range of power that the system can produce. Ideally this reduction in power can be reduced by improving the optical setup for this application, but this type of correction is still relevant for correcting unavoidable defects in any optical system utilizing a digital micromirror device [6].

The custom FEA thermal modeling framework was employed to predict the temperature profile within a 2.3 x 1.3 mm rectangular region. While the absolute values from the model are ideally expected to align with experimental results, an exact match is not critical for this work. Accurately modeling heat conduction and heat capacity is more important, as the normalized thermal gradient is used to calculate the correction mask. This profile was normalized by the highest temperature value, converting the profile into a greyscale image. The complement of this image was then used to generate an optical compensation mask for the DMD. This compensation mask was then input back into the thermal simulation as a power distribution map, resulting in a much more even temperature prediction, as displayed on the right side of the figure below.

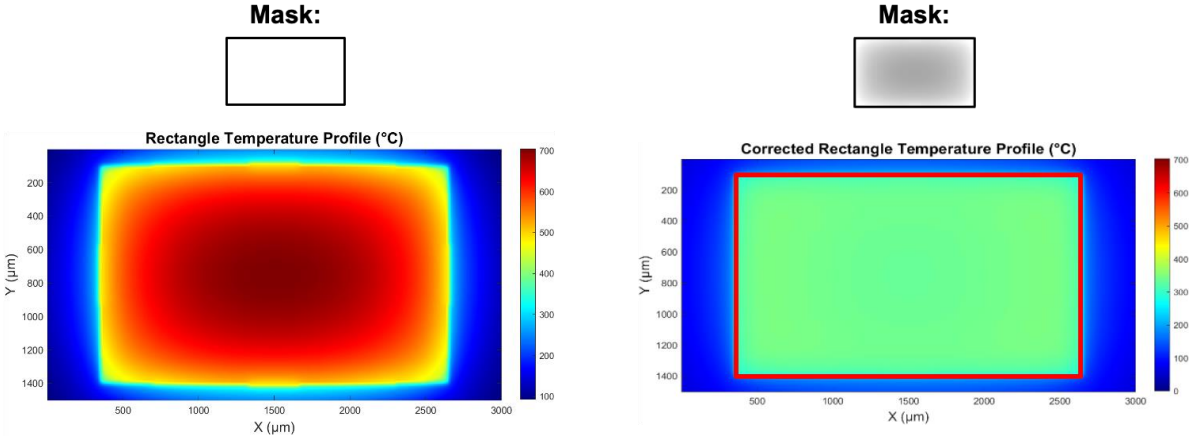

Figure 5: Temperature distributions generated by the thermal finite element analysis model for two different masks/heating profiles.

Finally, the optical and thermal correction masks were combined with the desired part image through two element-wise multiplication operations, producing the final modulated image used to evaluate the effectiveness of the correction approach. This composited image resulted in the final power being 70% of the unmodulated power. The test image used for this work was a 14 x 24 array of 50 µm circles, with the diameters of the parts

across the bed serving as an indicator of the effective temperature gradient. A smaller range and variance in the final part diameters indicate a more uniform temperature distribution.

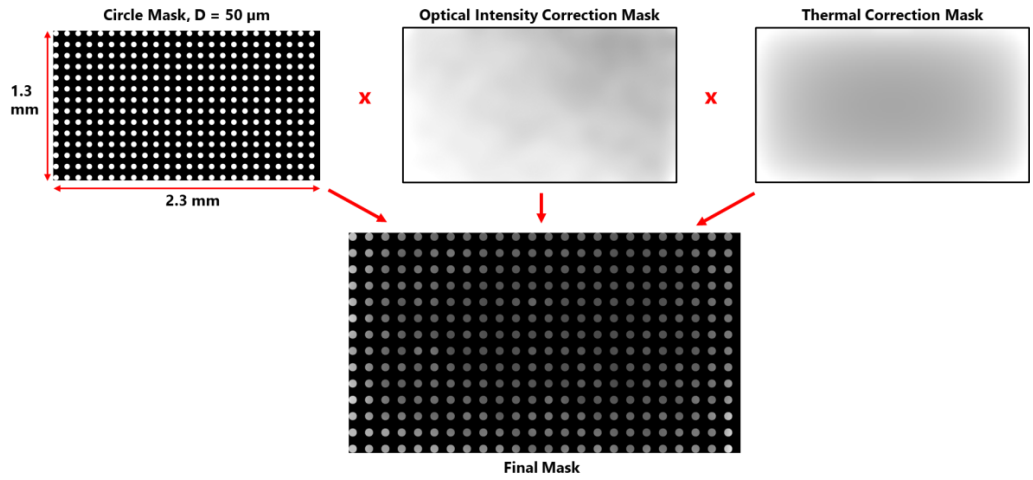

Figure 6: Process of creating the final mask by compositing 50 µm circle array image with the optical and thermal corrections through element-wise multiplication.

To analyze the effects of the modulation approach, 5 samples for both the modulated and unmodulated masks were created. The layer thickness of the particle bed used for these samples is approximately 1 µm thick and solvent is used to wash away unsintered nanoparticles on each sample for imaging. The laser power used for the modulated and unmodulated cases were 4.31 W and 2.85 W respectively and the laser is turned on for 2.5s. The discrepancy between power between the two cases is to keep the average power input for all samples the same as the modulation approach decreases the average intensity of the desired mask. Microscope images of the samples were taken, and the Hough circle transform algorithm was used to automatically determine the diameters of the circles in the images. The figure below illustrates the diameters of the circles across the frame for both the modulated and unmodulated masks.

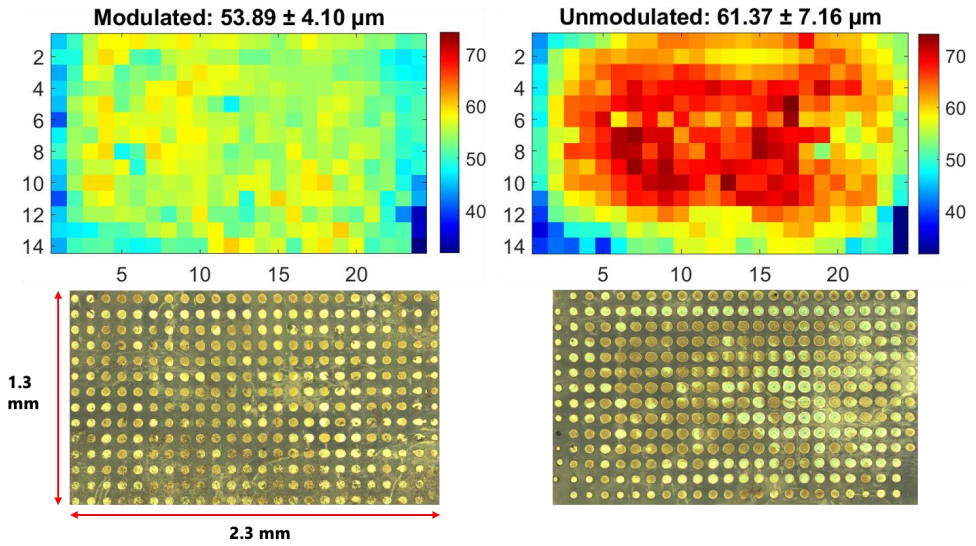

Figure 7: Heat maps comparing the size uniformity of circles produced by modulated and unmodulated masks. The average circle diameter produced at the position within the exposure frame is shown for both cases (n = 5).

The average diameter of the circles in the unmodulated case is 61.37 ± 7.16 µm vs the 53.89 ± 4.10 µm for the corrected case. Additionally, in the unmodulated case, the circles toward the center of the frame are significantly larger than those at the edges, with diameters up to 3.2 times greater than the smaller circles at the edges. Assuming that the distribution of diameters is Gaussian, centered physically at the middle of the exposure frame, the corrected approach has effectively reduced the thermal gradient across the frame by ~ 43%. A histogram showing the distribution of all the circles created across the 10 samples is presented below.

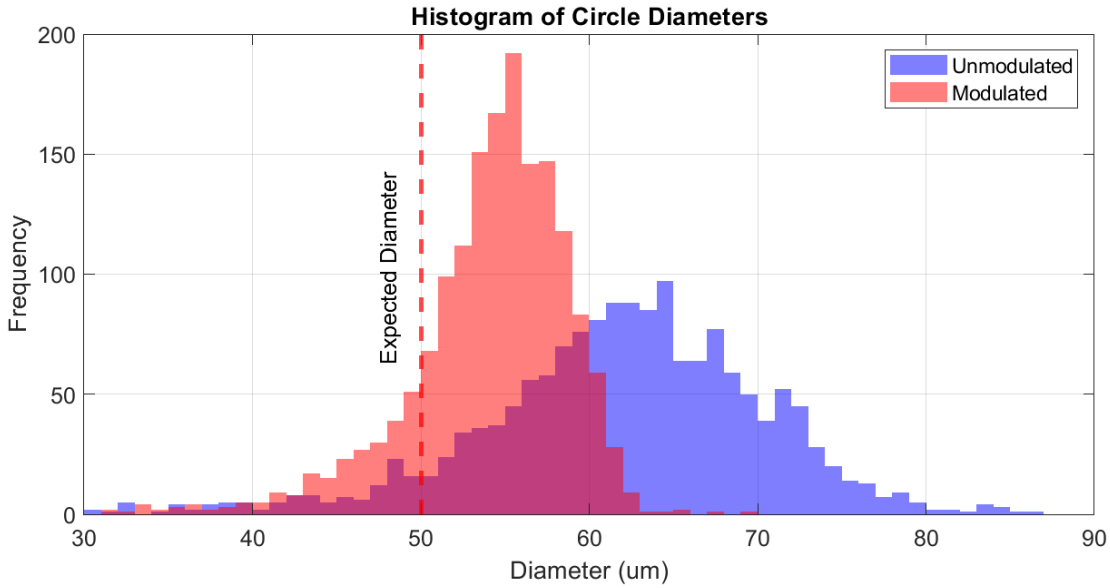

Figure 8: The histogram shows the distribution of circle diameters for both cases. The red histogram represents the distribution of diameters for parts created with the corrected mask, while the blue histogram shows the distribution for parts created with the uncorrected mask.

As shown in Figure 8 above, the modulated circles exhibit a much tighter distribution, closer to the expected diameter of 50 µm, compared to the unmodulated case. Combined with visual observation, this indicates a significant improvement in the uniformity of the circle diameters in the modulated case.

Conclusion

The objective of this work was to improve the process resolution of the µ-SLS system leveraging the intensity modulation capabilities of the digital micromirror device. A passive intensity modulation method, incorporating illumination correction and thermal gradient compensation based on temperature profiles from a thermal FEA model, was implemented to enhance part uniformity across the sintering region of the DMD. Using computational models to predict temperature gradients for a static mask is the first step in incorporating a full-scale sintering model used for any mask. Further model tuning can be done with this approach using the diameters as an indicator for thermal spread, allowing for the prediction of absolute temperatures which is crucial for more complex control techniques. The goal is to eventually project mask sequences with rapid and small changes to the intensity across each frame which will fully utilize the spatiotemporal modulation capability of the digital micromirror device. This future work will enable the system to correct for much control and adjust finer temperature gradients on the order of microns, as opposed to the millimeter-scale gradients addressed in this paper.

References

[1] N. K. Roy, D. Behera, O. G. Dibua, C. S. Foong, and M. A. Cullinan, "A novel microscale selective laser sintering (μ-SLS) process for the fabrication of microelectronic parts," *Microsyst Nanoeng*, vol. 5, no. 1, p. 64, Dec. 2019.

[2] D. Behera, A. Liao, and M. A. Cullinan, "Passive intensity modulation of a pattern for fabricating near-net shaped features in microscale metal additive manufacturing," *Manufacturing Letters*, vol. 35, pp. 63–67, Jan. 2023.

[3] J. Grose, O. G. Dibua, D. Behera, C. S. Foong, and M. Cullinan, "Simulation and Property Characterization of Nanoparticle Thermal Conductivity for a Microscale Selective Laser Sintering System," *ASME Journal of Heat and Mass Transfer*, vol. 145, no. 5, p. 052501, May 2023.

[4] J. Grose, A. Liao, C. Foong, and M. A. Cullinan, "Part-Scale Simulation of Heat Affected Zone Development and Part Formation in a Microscale Metal Additive Manufacturing System," 2024.

[5] H. Kim, J. Grose, A. Liao, C. Okwudire, and M. Cullinan, "A Model-based Control Framework for Microscale Selective Laser Sintering," Bellevue, WA: ASPE, 2022.

[6] J. Yoon, K. Kim, and W. Park, "Modulated grayscale UV pattern for uniform photopolymerization based on a digital micromirror device system," *Appl. Phys. Lett.*, vol. 111, no. 3, p. 033505, Jul.